

# Engineering biomimetic hair bundle sensors for underwater sensing applications

Kottapalli, Ajay Giri Prakash; Asadnia, Mohsen; Karavitaki, K. Domenica; Warkiani, Majid Ebrahimi; Miao, Jianmin; Corey, David P.; Triantafyllou, Michael

2018

Kottapalli, A. G. P., Asadnia, M., Karavitaki, K. D., Warkiani, M. E., Miao, J., Corey, D. P., & Triantafyllou, M. (2018). Engineering biomimetic hair bundle sensors for underwater sensing applications. AIP Conference Proceedings, 1965(1), 160003-. doi:10.1063/1.5038533

<https://hdl.handle.net/10356/88709>

<https://doi.org/10.1063/1.5038533>

---

© 2018 The Author(s) (Published by AIP). This paper was published in AIP Conference Proceedings and is made available as an electronic reprint (preprint) with permission of The Author(s) (Published by AIP). The published version is available at: [<http://dx.doi.org/10.1063/1.5038533>]. One print or electronic copy may be made for personal use only. Systematic or multiple reproduction, distribution to multiple locations via electronic or other means, duplication of any material in this paper for a fee or for commercial purposes, or modification of the content of the paper is prohibited and is subject to penalties under law.

*Downloaded on 13 Mar 2024 17:00:38 SGT*

# Engineering Biomimetic Hair Bundle Sensors for Underwater Sensing Applications

Ajay Giri Prakash Kottapalli<sup>1,a)</sup>, Mohsen Asadnia<sup>2,b)</sup>, K. Domenica Karavitaki<sup>3,c)</sup>,  
Majid Ebrahimi Warkiani<sup>4</sup>, Jianmin Miao<sup>5</sup>, David P. Corey<sup>3</sup>  
and Michael Triantafyllou<sup>6</sup>

<sup>1</sup>*Center for Environmental Sensing and Modeling (CENSAM) IRG Singapore-MIT Alliance for Research and Technology (SMART) Centre, Science Drive 2, 117543 Singapore.*

<sup>2</sup>*Department of Engineering, Macquarie University, Sydney, New South Wales 2109, Australia.*

<sup>3</sup>*Howard Hughes Medical Institute and Department of Neurobiology, Harvard Medical School, 220 Longwood Avenue, Boston, MA 02115, USA*

<sup>4</sup>*School of Mechanical and Manufacturing, Engineering, Australian Centre for NanoMedicine, University of New South Wales, Sydney, New South Wales 2052,*

<sup>5</sup>*School of Mechanical & Aerospace Engineering, Nanyang Technological University, 50 Nanyang Avenue, 639798 Singapore.*

<sup>6</sup>*Department of Mechanical Engineering, Massachusetts Institute of Technology, 77 Massachusetts Avenue, Cambridge, MA 02139, USA.*

<sup>a)</sup> Corresponding author: [ajay@smart.mit.edu](mailto:ajay@smart.mit.edu)

<sup>b)</sup> [mohsen.asadnia@mq.edu.au](mailto:mohsen.asadnia@mq.edu.au)

<sup>c)</sup> [domenica\\_karavitaki@hms.harvard.edu](mailto:domenica_karavitaki@hms.harvard.edu)

**Abstract.** We present the fabrication of an artificial MEMS hair bundle sensor designed to approximate the structural and functional principles of the flow-sensing bundles found in fish neuromast hair cells. The sensor consists of micro-pillars of graded height connected with piezoelectric nanofiber “tip-links” and encapsulated by a hydrogel cupula-like structure. Fluid drag force actuates the hydrogel cupula and deflects the micro-pillar bundle, stretching the nanofibers and generating electric charges. These biomimetic sensors achieve an ultrahigh sensitivity of 0.286 mV/(mm/s) and an extremely low threshold detection limit of 8.24  $\mu\text{m/s}$ . A complete version of this paper has been published [1].

## INTRODUCTION

Mechanosensory hair cells are not just limited to the lateral lines of fishes but are also found as sensors and transducers in various sensing systems in mammals. The hair bundles of the hair cells are a basic biological sensing system found in auditory and vestibular systems of all vertebrates [2]. It is rather surprising to notice a high level of functional overlap between the auditory hair cells found in the inner ears of mammals and the lateral-line hair cells found in fishes and amphibians. The intricate morphological organization of the hair bundle with varying heights of the stereocilia is rather complex and could be quite challenging to achieve through micro-fabrication techniques [1]. This could be the reason that among all the superficial neuromast (SN)-inspired flow sensors developed so far, the hair bundle has always been approximated as a cylindrical pillar [3-5]. Most of the researches developed artificial lateral-lines in the past undertook a bio-inspired approach by developing devices that emulate the flow sensing functionality of the SNs [6-9]. On a contrary, this paper presents a biomimetic approach to develop a novel flow sensor which attempts to replicate (within fabrication limits) the morphological organization and sensing principles

of the biological hair bundle. The tip-links that form the core sensing elements in the individual hair cell bundle act as sensing elements in the artificial ciliary bundle microelectromechanical (MEMS) device. Biomimetic materials that mimic the material properties of the biological cupula are identified and characterized through nano-indentation and rheological studies. Hydrogel micro-structures are developed through drop-casting and swelling to encapsulate the MEMS device thus mimicking the biological cupula.

### **MEMS Ciliary Bundle Sensor Structure**

The biomimetic MEMS ciliary bundle sensor presented in this work is designed on the same structural basis as that of the biological hair bundle. A bundle of high-aspect ratio polydimethylsiloxane (PDMS) pillars positioned close to each other approximates the geometrical arrangement of stereocilia within the biological hair bundle. Polyvinylidene fluoride (PVDF) nanofibers form the “tip-links” connecting all the consecutive tips of the pillars and a single tallest pillar that mimics the kinocilium. A soft-polymer cupula developed from hyaluronic acid methacrylic anhydride (HA-MA) acts as a cupula. The HA-MA hydrogel polymer encapsulates all the pillars. A very thin layer of conductive epoxy is used to form electrodes on both the sides of the artificial hair cell bundle for collecting signal generated from the nanofibers.

The MEMS ciliary bundle sensor consists of three major structural parts which are 1) a hydrogel cupula that interacts with the external flow, 2) pillars that transduce the flow to the PVDF nanofibers, and 3) PVDF nanofibers that are the actual sensing elements. The following sections describe the design and dimensions of these sub-components of the MEMS flow sensor (Fig. 1).

The artificial ciliary bundle consists of 55 PDMS pillars arranged into 10 rows of graded height and a single tallest pillar (“kinocilium”). Pillars in each row have the same height and the height of pillars in successive rows decreases as the distance from the tallest pillar increases (Fig. 1b). Each pillar of a successive row of higher height falls at the center of the two pillars of the preceding shorter row. This arrangement maximizes the number of PVDF nanofibers generated between the pillars and ensures that all the fibers have similar length, which is equal to the distance between the rows. This arrangement and dimensional design of the pillars is inspired by the studies on the biological hair bundle [10, 11]. Each PDMS pillar has a diameter of 50  $\mu\text{m}$  and successive pillars are spaced at 25  $\mu\text{m}$  distance. The entire distance between the tallest pillar and the shortest pillar is 725  $\mu\text{m}$ . Although the size of the biological hair bundles is much smaller, the dimensions of the artificial pillars are chosen to be feasible for fabrication through micro-lithographic techniques and PDMS molding processes. The graded height increment of the PDMS pillars ranges from 200  $\mu\text{m}$  to 400  $\mu\text{m}$  for the tallest pillar. The PVDF nanofibers are formed through an electrospinning process. Aligned PVDF nanofibers stretch from the shortest to the longest pillar in such a way that they contact all the pillars due to the gradually increasing height gradient. Just the way the ion channels in the biological hair bundle form the basic sensing elements of the neuromast, the PVDF nanofibers are the actual sensing components of the MEMS flow sensor. PVDF was chosen due to its high piezoelectric coefficient and capacity to form nanofibers through an electrospinning process. PZT nanofiber exhibits a higher piezoelectric coefficient than PVDF however it is a ceramic material and the fibers generated are not flexible leading to breakage during sensor operation [12]. Stretching of the nanofiber generates charges due to the piezoelectric nature of PVDF material, which are collected as output voltage. It is very important to ensure that during the electrospinning process the nanofibers connect all the pillars and do not simply bridge the shorter pillars with the tallest pillar. In addition, ensuring that all nanofibers have the same length is crucial for the device performance and ensures device-to-device repeatability of flow calibrations.

HA-MA hydrogel is identified as a material with close properties to the biological cupula [13]. The hydrogel cupula not only interacts with the flow and couples the flow generated drag force to the embedded pillars but also acts as a package protecting the fragile nanofibers [14]. The presence of the hydrogel cupula enhances the sensitivity of the MEMS flow sensor in many ways. The height and diameter of the hydrogel cupula is larger than those of the pillars, thereby an increased surface area projected to the flow results in enhanced sensitivities. The enhanced height of the cupula over the pillars causes the structure to extend beyond the boundary layers generated by the flow leading to a higher sensitivity. The HA-MA hydrogel material has a density close to the density of water and is mainly driven through viscous forces. The cupula diminishes the effects of high frequency flows and Brownian motion thereby increasing the signal to noise ratio of the MEMS flow sensors. The hydrophilicity and permeability of hydrogel material enhances the signal absorption through an enhanced friction factor associated with the material [15, 16].

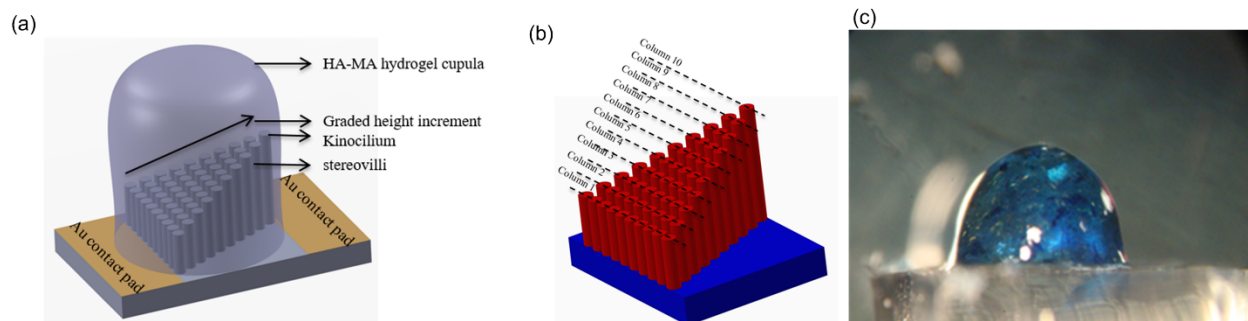


**FIGURE 1.** Artificial hair bundle design. a) Schematic describing the artificial hair bundle structure and the various materials used in the device fabrication. b) Schematic showing the number of pillars and their organization in each biomimetic MEMS sensor. c) Optical image of the artificial MEMS hair bundle sensor encapsulated by the cupula-like HA-MA hydrogel.

## Experimental Characterization of the MEMS Flow Sensor

The goal of the characterization is to determine the sensitivity, threshold sensing limits and the sensing accuracy of the sensor. Experiments to determine the direction dependence of the sensor output are also illustrated in this section. Unlike other piezoelectric sensors fabricated using bulk piezoelectric material, these sensors do not need to be poled with high electric field. This is because the polling is conducted in situ while the electrospinning process applies high electric field to generate nanofibers. In order to tap the output voltage generated by the sensor two probes are connected to the contact pads as shown in Fig. 2a. In all the experiments, a dipole (vibrating sphere of 8 mm diameter) stimulus is used to generate oscillatory flows of various amplitudes and frequencies underwater. The experimental results section is divided into three main experiments. The first and the basic experiment is to determine if the MEMS ciliary bundle sensor responds to various frequencies of the oscillatory flows generated by the dipole. The second experiment is to calibrate the sensor output to various flow velocities generated by the dipole. The third experiment determines the direction dependence of the output of the MEMS sensor for various angles in which the dipole is positioned with respect to the sensor. In all the experiments, the output of the sensor is acquired using National Instruments Data Acquisition (NI-DAQ) card and recorded in LABVIEW. The following sections explain the experimental results pertaining to these three classifications.

The response of the sensor to a dipole vibrating at 2Hz and 35Hz is evaluated. The dipole is set to vibrate using a permanent magnet mini-shaker (model 4810, B&K, Norcross, GA, USA). The dipole is connected to the membrane of the mini-shaker by a stainless steel rod 120 mm long and 2 mm in diameter. The dipole can be driven at a desired amplitude and frequency controlled by a function generator connected to the mini-shaker. The signal from the function generator is amplified by a specified gain through a power amplifier (type 2718, B&K). The mini-shaker is inverted and mounted on top of a water tank of dimensions 1 m (L)  $\times$  0.6 m (W)  $\times$  0.4 m (H) so that the dipole is immersed 120 mm deep into water. In all the experiments, the output from the sensors is amplified 500 times using a SRS560 low-noise pre-amplifier. The dipole is positioned 25 mm away from the sensor and is vibrated such that the direction of vibration is parallel to the long-axis of the pillars. The vibration of the dipole displaces water molecules surrounding the dipole. The vibrating dipole generates a pressure profile which displaces water in the vicinity of the dipole at the same frequency as that of the dipole. These pressure variations cause the cupula of the MEMS sensor to vibrate. The vibration of the cupula is transduced into displacements of the pillars, which in turn causes the nanofiber “tip-links” to expand and contract generating the sensor output. Figure 2b shows the output of the sensor to a dipole vibrating at 2Hz.

The dipole stimulus is calibrated to determine the velocity of vibration for various sinusoidal signal amplitudes using a LDV. In order to determine the sensitivity and velocity detection threshold of the sensor, the vibration of the dipole is varied from 1 $\mu$ m/s to 80mm/s. The dipole is vibrated with a frequency of 35Hz and the amplitude of the vibration is varied to generate varying flow velocities. The sensor is positioned 25mm from the dipole and the output of the sensor is amplified 500 times using a SRS low-noise pre-amplifier. Figure 2c shows the flow velocity calibration of the sensor. The results presented are average results of 5 runs. The sensor’s output varies linearly with respect to the amplitude of the sinusoidal source signal as expected. The sensor demonstrates a threshold sensing limit of 8.24 $\mu$ m/s below which the sensor’s response starts to become noisy because the sensor output is hitting the

noise floor. The sensor demonstrates a sensitivity of 0.286 mV/(mm/s) for sensing water flow. The threshold sensing limit achieved by this sensor is extremely low even compared to that of the biological neuromast counterpart. In Fig. 2c it can be observed that the linear increase in sensor output is very gradual for water flow velocities up to 20mm/s, after which, the rate of increase of sensor output is much higher. This is due to a skin friction on the standing pillar, generated at velocities below 20mm/s (corresponding to a Reynold's number  $R_e \approx 50$ ), that majorly contributes to the sensor output. At velocities below 20mm/s, the drag force that contributes to the output is linear to flow velocity. However, at higher velocities, the pressure-gradient dominates in the overall contribution to the sensor output.

In order to determine the direction dependence of the sensor output, the position of the dipole is shifted at various angles with respect to the MEMS hair cell bundle. Figure 2d shows the various directions for which the sensor's output is experimentally acquired. The sensor shows a huge variation in output as the dipole is shifted from  $0^\circ$  to  $180^\circ$ . The best performance case of the sensor is  $0^\circ$  when the sensor shows a maximum voltage output. This is because at  $0^\circ$  orientation the nanofiber tip-links are stretched to the maximum extent. At  $180^\circ$  the sensor does not generate any output because at  $180^\circ$  the nanofiber tip-links slack and do not experience any stress thereby do not generate any output voltage. In directions between  $0^\circ$  and  $180^\circ$ , the sensors output varies as a cosine function of the orientation. These results match very well with the predictions on the direction detection ability of the biological hair bundle sensors.

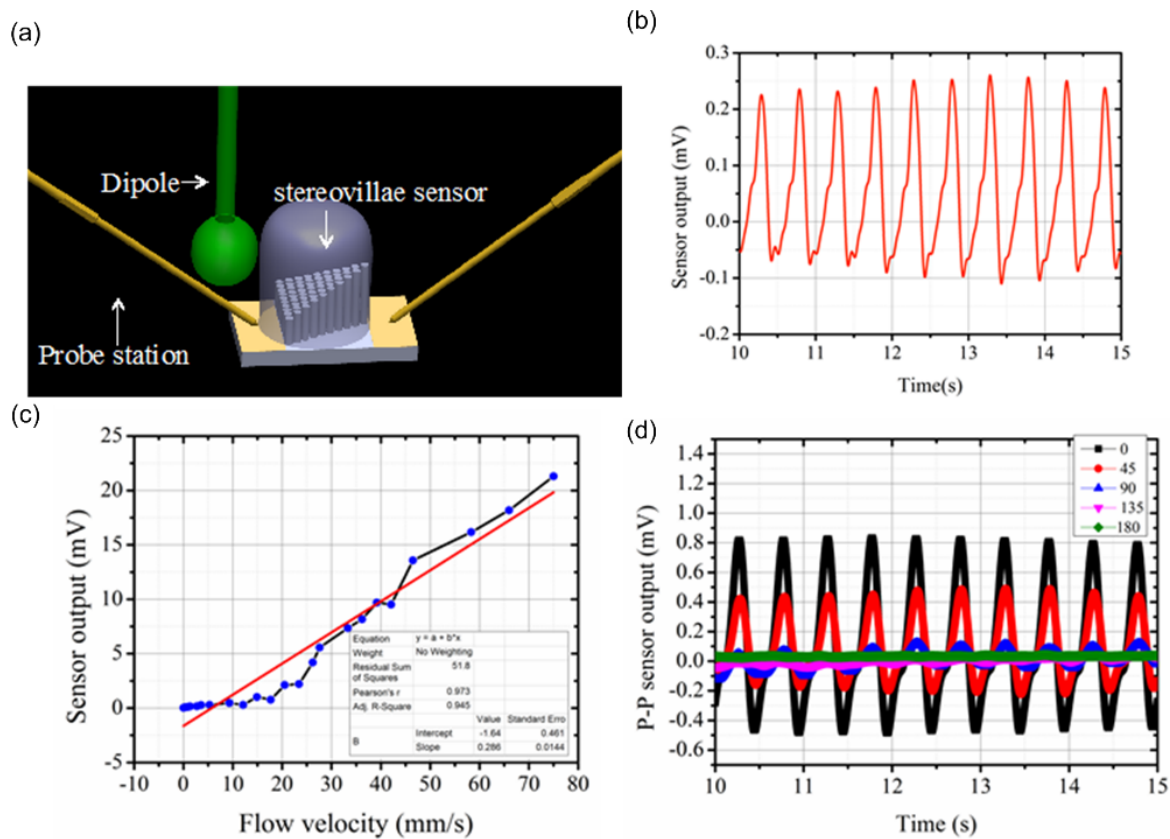


**FIGURE 2.** a) Experimental set-up showing probes that connect to the contact pads of the artificial hair bundle sensor and the dipole in the vicinity of the sensor. B) Sensor outputs for dipole stimulus vibrating at 2Hz. c) Flow velocity calibration of the MEMS sensors. d) Directional dependence of the sensor output.

## SUMMARY

In this paper we describe the fabrication of an artificial ciliary bundle which is the closest biomimetic to the biological hair cell bundle developed to date. The device consists of 55 PDMS pillars organized into 10 rows of graded heights. The PDMS pillars are interconnected through piezoelectric PVDF nanofiber “tip-links”. These PVDF nanofibers are aligned from the shortest pillars to the tallest pillar and are developed through an electrospinning process. An HA-MA hydrogel cupula is developed through a drop-casting process and encapsulates all the pillars and the nanofibers. Since all the PDMS pillars are infused into the hydrogel cupula, the bending of the cupula causes all the pillars to bend. Due to the different heights of the pillars in each row of the bundle, there is a difference in the displacement of the pillars of various rows, and a resultant stress induced on to the PVDF nanofibers that connect the pillars. This stress causes a voltage output that is acquired. The sensors are calibrated for underwater flow velocity sensing using a dipole stimulus. The sensors demonstrated a high sensitivity of 0.286 mV/(mm/s) and an extremely low threshold detection limit of 8.24 $\mu$ m/s.

## ACKNOWLEDGEMENTS

This research is supported by the National Research Foundation (NRF), Prime Minister’s Office, Singapore under its Campus for Research Excellence and Technological Enterprise (CREATE) programme. The Center for Environmental Sensing and Modeling (CENSAM) is an interdisciplinary research group (IRG) of the Singapore MIT Alliance for Research and Technology (SMART) centre. This research is also supported by the MIT Sea Grant College Program.

## REFERENCES

1. M. Asadnia, A. G. P. Kottapalli, K. D. Karavitaki, M. E. Warkiani, J. Miao, D. P. Corey, et al., [Scientific Reports](#) **6** (2016).
2. D. E. Jaalouk and J. Lammerding, [Nature Reviews Molecular Cell Biology](#) **10**, 63-73 (2009).
3. M. Asadnia, A. G. P. Kottapalli, J. Miao, M. E. Warkiani, and M. S. Triantafyllou, [J. R. Soc. Interface](#) **12**, 20150322 (2015).
4. M. J. McHenry and S. M. van Netten, [J. Exp. Biol](#) **210**, 4244-4253 (2007).
5. A. P. Kottapalli, M. Asadnia, J. Miao, and M. Triantafyllou, Micro Electro Mechanical Systems (MEMS), IEEE 26th International Conference on, 25-28 (2013).
6. L. D. Chambers, O. Akanyeti, R. Venturelli, J. Ježov, J. Brown, M. Kruusmaa, et al., [J. R. Soc. Interface](#) **11**, (2014).
7. J. Dusek, A. G. P. Kottapalli, M. E. Woo, M. Asadnia, J. Miao, J. H. Lang, et al., [Smart Mater. Struct.](#) **22** (2013).
8. M. E. McConney, N. Chen, D. Lu, H. A. Hu, S. Coombs, C. Liu, V. V. Tsukruk, [Soft Matter](#), **5**, 292-295, (2009).
9. A. G. P. Kottapalli, M. Asadnia, J. Miao, and M. Triantafyllou, [J. Intell. Mater. Syst.](#) **26**, 38-46 (2015).
10. S. Coombs, [J. Exp. Biol.](#) **190**, 109-129 (1994).
11. J. H. Nam, J. R. Cotton, E. H. Peterson, W. Grant, [Biophysical Journal](#) **90**, 2786-2795 (2006).
12. J. Chang, M. Domnner, C. Chang, and L. Lin, [Nano Energy](#), **1**, 356-371, (2012).
13. M. Asadnia, A. G. P. Kottapalli, R. Haghighi, A. Cloitre, P. V. y Alvarado, J. Miao, M. Triantafyllou, [Bioinspir. Biomim](#) **10**, 036008 (2015).
14. M. E. McConney, N. Chen, D. Lu, H. A. Hu, S. Coombs, C. Liu, et al., [Soft Matter](#) **5**, 292-295 (2009).
15. M. E. McConney, K. D. Anderson, L. L. Brott, R. R. Naik, and V. V. Tsukruk, [Adv. Funct. Mater.](#) **24**, 2527-2544 (2009).
16. K. D. Anderson, D. Lu, M. E. McConney, T. Han, D. H. Reneker, and V. V. Tsukruk, [Polymer](#) **10**, 5284-5293 (2008).



## COMMENTS & QUESTIONS

[Online Forum]

**Dáibhid Ó Maoiléidigh:** 1. I like this attempt to create an artificial neuromast, but the authors should describe the differences between the geometry of their artificial system and a real neuromast. Some differences that come to mind are: neuromasts consist of several pairs of hair cells with the hair bundles in each pair pointing in opposite directions; the kinocilium of these hair cells is several-fold taller than the tallest stereocilium; and the number of stereocilia in each row are roughly equal.

2. Because the output of the sensor is amplified 500-fold by a pre-amplifier, it is not true that the sensitivity is 0.287 mV/(mm/s). The voltage sensitivity of the sensor is 500 times less than this.

3. The Reynold's number for hair bundles in vivo is less than 1. Do you plan to change your sensor to match this regime?

4. Does the dipole create a displacement source or a pressure source, or does the dipole's displacement depend on the presence of the artificial neuromast?

5. What does it mean when you say that the dipole is driven by a sinusoidal signal of amplitude 250mVrms? You don't describe how the dipole is driven. What is the dipole's amplitude of motion?

6. The fibers are not perfectly parallel, so the response to 180 degree dipole stimulation should not be exactly zero.

Author: Dáibhid, thank you for thoroughly reading the paper and for your comments. All minor comments have been incorporated in the document. Here are responses to major comments:

1. This was not an attempt to create an artificial neuromast; we have corrected any text that was misleading in that direction. Rather this is an attempt to create an artificial flow sensor by mimicking the anatomy of a vestibular-like hair bundle. Certain geometrical aspects of the pillars i.e. the height of the kinocillium-like pillar with respect to the rest of the pillars, and the number of pillars in each row have been mainly limited by the fabrication capabilities.

2. You are right. However, in the MEMS flow-sensor literature, the sensitivity is mentioned together with the value of the amplification. Therefore, we have also stated the value of the amplification in the paper.

3. The dimensions of the MEMS sensor demonstrated in this work are much larger than those of the biological hair bundle. In future versions of the sensor, we plan to reduce these dimensions. However, there are constraints on how small we can fabricate the device due to limitations posed by the lithographic processes in nanofabrication.

4. The vibrating dipole acts as an oscillatory flow source. When the dipole vibrates in water, it displaces the surrounding water and the water moves around the dipole into the region that has just vacated. For simplicity, we neglected the water displacements that occur due to gravity, temperature differences and rotational motion; we only considered the flow generated due to the movement of the dipole. The periodic vibration of the dipole exerts pressure on the MEMS sensor, which in turn responds by generating a voltage output that contains the details of the inherent flow frequency and amplitude. The dipole's displacement does not depend on the presence of the artificial hair-bundle as the dipole is forced to vibrate through a mini shaker that drives it.

5. The dipole is driven through a mini shaker connected to a function generator. The voltage amplitude applied to the mini shaker through the function generator causes a physical displacement of the dipole, which then generates flow. We have expanded the experimental characterization section to describe how the dipole is driven and to clarify the driving signal amplitude.

6. Yes, the output of the MEMS sensor should not be exactly zero. In fact, this is exactly what is seen in the sensor testing. However, the output is much lower than in cases when the flow is at angles <180 degrees.